Chemistry & Biology 13, 779–786, July 2006 DOI 10.1016/j.chembiol.2006.05.015

A General Strategy for Creating "Inactive-Conformation" Abl Inhibitors

Barun Okram,[1,4] Advait Nagle,[2,4] Francisco J. Adrián,[2] Christian Lee,[2] Pingda Ren,[2] Xia Wang,[2] Taebo Sim,[3] Yongping Xie,[2] Xing Wang,[2] Gang Xia,[2] Glen Spraggon,[2] Markus Warmuth,[2] Yi Liu,[2,*] and Nathanael S. Gray[2,3,*]

[1] Department of Chemistry and the Skaggs Institute for Chemical Biology
The Scripps Research Institute
10550 North Torrey Pines Road
La Jolla, California 92037

[2] Genomics Institute of the Novartis Research Foundation
Department of Biological Chemistry
10675 John Jay Hopkins Drive
San Diego, California 92121

[3] Harvard Medical School
Dana Farber Cancer Institute
Department of Biological Chemistry and Molecular Pharmacology
Seeley G. Mudd Building, 628A
250 Longwood Avenue
Boston, Massachusetts 02115

Summary

Kinase inhibitors that bind to the ATP cleft can be broadly classified into two groups: those that bind exclusively to the ATP site with the kinase assuming a conformation otherwise conducive to phosphotransfer (type I), and those that exploit a hydrophobic site immediately adjacent to the ATP pocket made accessible by a conformational rearrangement of the activation loop (type II). To date, all type II inhibitors were discovered by using structure-activity-guided optimization strategies. Here, we describe a general pharmacophore model of type II inhibition that enables a rational "hybrid-design" approach whereby a 3-trifluoromethylbenzamide functionality is appended to four distinct type I scaffolds in order to convert them into their corresponding type II counterparts. We demonstrate that the designed compounds function as type II inhibitors by using biochemical and cellular kinase assays and by cocrystallography with Abl.

Introduction

There are 518 kinases encoded in the human genome, and they have been demonstrated to play pivotal roles in virtually all aspects of cellular physiology [1]. Misregulation of kinase activity has been implicated in pathological conditions ranging from cellular transformation in leukemias to neuronal disorders. Hyperactivated kinases that are no longer subject to normal physiological constraints result from activating point mutations, formation of constitutively active fusion proteins, loss of negative regulators, and excessive stimulation by extracellular growth factors [2–5]. New classes of selective kinase inhibitors are urgently needed as "tools" to decipher the biological function of the large number of still uncharacterized kinases and as starting points for the development of drugs targeting therapeutically relevant kinases.

The highly conserved kinase domain consists of a bilobed structure, with Mg-ATP binding in a deep cleft located between the two lobes. The vast majority of small-molecule kinase inhibitors developed to date target the ATP binding site (type I inhibitors), with the kinase assuming a conformation almost identical to that used to bind ATP. Typically, type I inhibitors form between one and three hydrogen bonds to the backbone hinge amino acid residues that connect the N- and C-terminal lobes of the kinase domain [6]. Although some highly selective members of this class have been discovered, the highly conserved nature of the ATP binding region often results in type I inhibitors exhibiting poor kinase selectivity. The majority of type I inhibitors have been derived from leads discovered by using biochemical kinase assays performed at low ATP concentrations. These conditions favor the discovery of hydrophobic compounds that bind to the nucleotide binding pocket.

Fortunately, serendipity allowed for the identification of a second broad class of kinase inhibitors that preferably inhibits the inactive conformation of the kinase, thereby preventing its activation (Figure 1). This inactive conformation was first observed crystallographically in an inactive conformation of an unliganded insulin receptor kinase [7], but it was not until the structures of Abl in complex with imatinib and analogs were solved that it became clear that this conformation could be exploited by inhibitors [8–10]. This second broad class of kinase inhibitors (type II) utilizes the ATP binding cleft and an immediately adjacent hydrophobic pocket that is created when the activation loop, which contains the conserved DFG motif, is in an *out* conformation. The resulting *DFG-out* conformation is termed the "inactive conformation" because the amino acids in the ATP pocket are not oriented in a manner that would allow phosphotransfer to be catalyzed and the activation loop is in a conformation that blocks the approach of ATP and the substrate. Several distinct inhibitors, such as imatinib [9], BIRB796 [11], sorafenib [12], AAL993 [13], and others [14–16], have been crystallographically proven to be type II inhibitors.

A third broad class of kinase inhibitors that modulate kinase activity by binding at sites remote from the ATP cleft can be recognized. To date, only a few compounds have been disclosed that operate by this mechanism: the MEK inhibitors PD098059, PD184352, and U0126 [17–19]; the glucose kinase activator TDZD [20]; the IKK inhibitor BMS345541 [21]; the non-ATP-competitive Abl inhibitor GNF-2 [22]; the plekstrin homology domain-dependent Akt inhibitors Akt-I-1,2 [23]; and the Plk inhibitor ON01910 [24].

Here, we describe a simple chemical strategy for converting four known type I inhibitors into corresponding

*Correspondence: yliu@gnf.org (Y.L.); nathanael_gray@dfci.harvard.edu (N.S.G.)

[4] These authors contributed equally to this work.

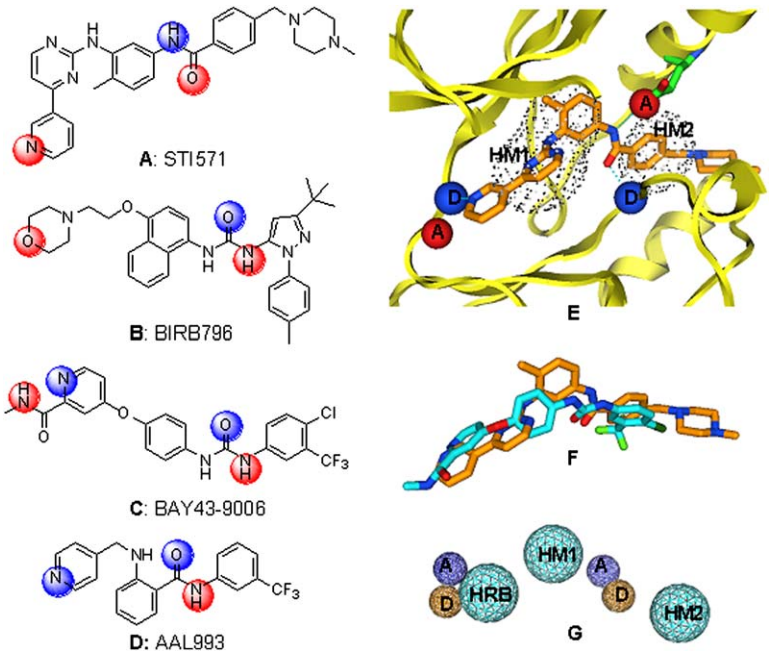

Figure 1. Recognizing "Type II" Inhibitors

(A–D) Chemical structures of imatinib (ST1571), BIRB796, sorafenib (BAY43-9006), and AAL993 highlighting the conserved hydrogen bond accepting (red circles) and donating (blue circles) interactions inferred by crystallography.

(E) Imatinib (gold) bound to Abl (yellow ribbon).

(F) Overlapping view of imatinib (gold) and sorafenib (blue) showing the molecular mimicry of the two.

(G) Pharmacophore model of a type II inhibitor.

A, D = hydrogen bond acceptor, donor; HRB = hinge region binder; HM1, 2 = hydrophobic motif 1, 2.

type II inhibitors with different kinase selectivity profiles and exceptionally potent cellular activity.

Results

In order to develop a general pharmacophore model for type II kinase inhibitors, we searched for structural features conserved in all known type II inhibitor kinase costructures. This analysis revealed that the majority of type II inhibitors made two pairs of conserved hydrogen bonds to their respective kinase targets: one pair to the hinge region amino acid and a second pair to the side chain carboxylate of a conserved glutamate in the α-C helix and to the backbone NH of the aspartate located in the DFG motif [8, 10]. In addition, all of the inhibitors had a hydrophobic substitution that occupied the region normally utilized by the phenyl ring of the phenylalanine of the DFG motif in the active conformation. The cocrystal structures revealed that despite the distinct chemical structures of the type II inhibitors, the distance between the hydrogen bond donor and acceptor functionality is highly conserved (Table 1). These observations can be combined to create a general pharmacophore model for a type II kinase inhibitor (Figure 1).

Inhibitor Design Strategy

We hypothesized that we could convert known type I inhibitors into type II inhibitors by appending a second hydrogen bonding pair and hydrophobic motif onto a type I scaffold. To test this hypothesis, we selected four type I inhibitors from distinct scaffold classes (**1**, **4**, **7**, and **11**) and introduced a 3-trifluoromethylbenzamide substituent at a position that molecular modeling predicts would mimic the placement of the same moiety in sorafenib (BAY43-9006) to generate four classes of potential type II inhibitor scaffolds (**2**, **5**, **8**, **9**, **12**, and **14**; Figure 2). The four type I scaffolds were chosen because of their high structural similarity to compounds whose binding mode to kinases has been determined by X-ray crystallography or on the basis of molecular modeling, which allowed us to predict the optimal attachment site for the 3-trifluoromethylbenzamide. For example, compound **1** was derived from the phenylamino pyrimidine class [25], which were the lead structures for the development of the known type II inhibitor imatinib, and it is expected to form a hydrogen bond from pyridine nitrogen to the kinase hinge (cocrystal of Gleevec with *c*-Abl; PDB code: 1IEP). Alternatively, based on the closely related CDK inhibitors (cocrystal of human CDK2 with various small-molecule inhibitors; PDB codes: 1PXM, 1PXN, 1PXO, and 1PXP) [26], compound **1** could also form a pair of hydrogen bonds from the pyrimidine N1 and 2-NH to the kinase hinge region. The second scaffold, **4**, was designed as a simplified version of the pyrrolopyrimidine Jak-3 inhibitor CP690550 [27], and it is expected to form a pair of hydrogen bonds from N1 and the 9-NH to the kinase hinge (cocrystal of B-Raf with BAY43-9006; PDB code: 1UWH). The tricyclic inhibitor **7** was designed based on the structurally related p38 MAP kinase inhibitor [28], and it is expected to bind to the kinase hinge by using the same functionality as compound **4**. Pyrido[2,3-*d*]pyrimidine compound **11** is an example of a well-characterized dual Src/Abl inhibitor that has been recently shown to inhibit a subset of

Table 1. Distance and Bond Number between the H Bond Acceptor in the Hinge Region and the Second H Bond Acceptor in the DFG Motif of Four Known Type II Inhibitors

Inhibitor	Distance between Hinge Acceptor and DGF-Motif Acceptor (Å)	Number of Bonds between Hinge Acceptor and DGF-Motif Acceptor
Imatinib	10.0	12
BIRB796	9.7	12
Sorafenib	8.8	11
AAL993	7.3	9

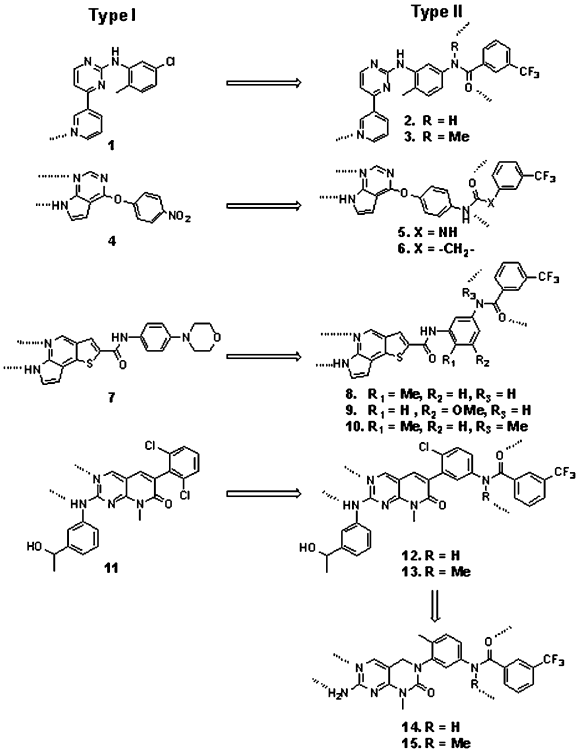

Figure 2. Chemical Structures of Four Classes of Designed Type II Inhibitors and Their Respective Type I Progenitors

Presumed hydrogen bonds are shown as dashed lines.

imatinib-resistant Bcr-Abl mutants (cocrystal of *c*-Abl with PD173955; PDB code: 1M52) [29, 30]. We use four lines of evidence to suggest that the type II inhibitors bearing 3-trifluoromethylbenzamide bind to kinases differently than their progenitor type I scaffolds. First, the 3-trifluoromethylbenzamide-containing structures display significantly altered kinase selectivity in enzymatic and cellular assays. Second, for the compounds with activity against Abl kinase, we demonstrate that the type II inhibitors show a trend toward greater potency against dephosphorylated versus phosphorylated Abl. Third, we demonstrate the importance of the hydrogen bond-donating group formed by the amide (or urea) for obtaining potent kinase inhibition. Fourth, we have obtained a cocrystal of compound **14** with the catalytic domain of Abl, which demonstrates that it binds to the enzyme with an activation loop in the "DFG-out" conformation (type II mode).

Biochemical Kinase Selectivity

All of the compounds were tested against a panel of 59 recombinant serine/threonine and tyrosine kinases at a concentration of 1 or 10 μM (Figure 3). As illustrated in Figure 3, all of the type I and II inhibitor pairs (**1** versus **2**, **4** versus **5**, **7** versus **8**, and **11** versus **12**) exhibit significant differences in kinase selectivity. Three of the type I inhibitors exhibit only weak inhibitory activity (IC_{50} > 1 μM) on a limited number of kinases in the panel: **1** on c-Kit, Fms, KDR, Aurora A, Gsk3β, and Tie2; **4** on Jak2 and FGFR3; **7** on Jak2 and Tie2. Consistent with a close analog reported in the literature [29], the fourth type I inhibitor, **11**, exhibited potent pan-tyrosine kinase inhibitory activity as well as activity against serine/threonine kinases such as c-Raf, MAPK1, Aurora A, Jak 2&3, Nlk, and c-Met. In contrast, each type II inhibitor exhibited significantly altered selectivity. For example, **2**, which has a structure highly similar to imatinib and nilotinib, exhibited enzymatic inhibitory activity against Abl, Blk, Brk, c-Kit, c-Src, Lck, PDGFR-α, c-Raf, Fms, Fyn, TrkB, and Sapk2a. The type II inhibitor, **5**, which is structurally similar to sorafenib, exhibited a very broad biochemical inhibitory profile inhibiting Alk, Aurora A, Flt3, Jak2, Fyn, Ron, p70S6K, and Ros kinases in addition to the kinases targeted by the phenylaminopyrimidine **2**. The type II inhibitor **8** also was more potent and displayed a broader kinase selectivity than its progenitor **7**. It was also capable of inhibiting *c*-Raf, Abl, Aurora A, Lck, Fms, PDGFR-α, KDR, Sapk2a, TrkB, Jak2, and, to a lesser, extent c-Kit, MAPK1, and Tie2. The fourth type II inhibitor, **12**, also exhibited altered selectivity relative to its progenitor, **11**, albeit to a lesser extent than the previous three compound pairs due to the already poor selectivity of **11**. These dramatic alterations in both selectivity and potency would suggest that each pair recognizes the kinase active site through fundamentally different binding modes. Although three of the newly created type II inhibitors (**2**, **5**, and **8**) inhibited more kinases than their type I counterparts (**1**, **4**, and **7**), we discovered that small alterations could be made to the type II inhibitors to create highly selective inhibitors. This is exemplified by the replacement of the urea of **5** with an amide in **6**, which resulted in a dramatic improvement in selectivity; **6** only significantly inhibited Flt3, Fms, PDGFR-α, KDR, and TrkB. These results suggest that the type II inhibitors **2**, **5**, **6**, **8**, and **12** can be viewed as core scaffolds that can be further elaborated to obtain inhibitors with the desired spectrum of inhibitory activities.

Cellular Kinase Selectivity

As there are frequently discrepancies observed between kinase inhibition measured by using biochemical versus cellular kinase assays, we evaluated the inhibitors in kinase-dependent cellular proliferation assays [31]. We utilized a cellular system in which murine Ba/F3 cells are transformed with 30 different constititutively active Tel-tyrosine kinase fusions to render them capable of growth in the absence of cytokine (IL-3) [31]. Selective kinase inhibition results in a blockade of cellular proliferation that can be discriminated from nonspecific cytotoxicity by comparison to inhibition of untransformed Ba/F3 cells or by reversal of compound-induced inhibition with cytokine (IL-3). As expected from the biochemical assays, three of the type I inhibitors (**1**, **4**, and **7**) exhibited no cellular activity on any of the kinases at a concentration below 1 μM; however, compounds **1** and **7** exhibited some activity below 5 μM (**1**: KitQ = 2.0 μM; **7**: Ros = 1.6 μM). In agreement with published data of a close analog, the pyridopyrimidinone **11** exhibited potent inhibition of Bcr-Abl (IC_{50} = 4 nM), Flt3 (IC_{50} = 1791 nM), and PDGFR-β (IC_{50} = 100 nM). In stark contrast, the corresponding type II analog, **12**, exhibited potent inhibition across the entire panel, which may result in part from cytotoxicity to parental Ba/F3 cells (IC_{50} = 300 nM). However, all other putative type II inhibitors displayed very potent cellular activities as

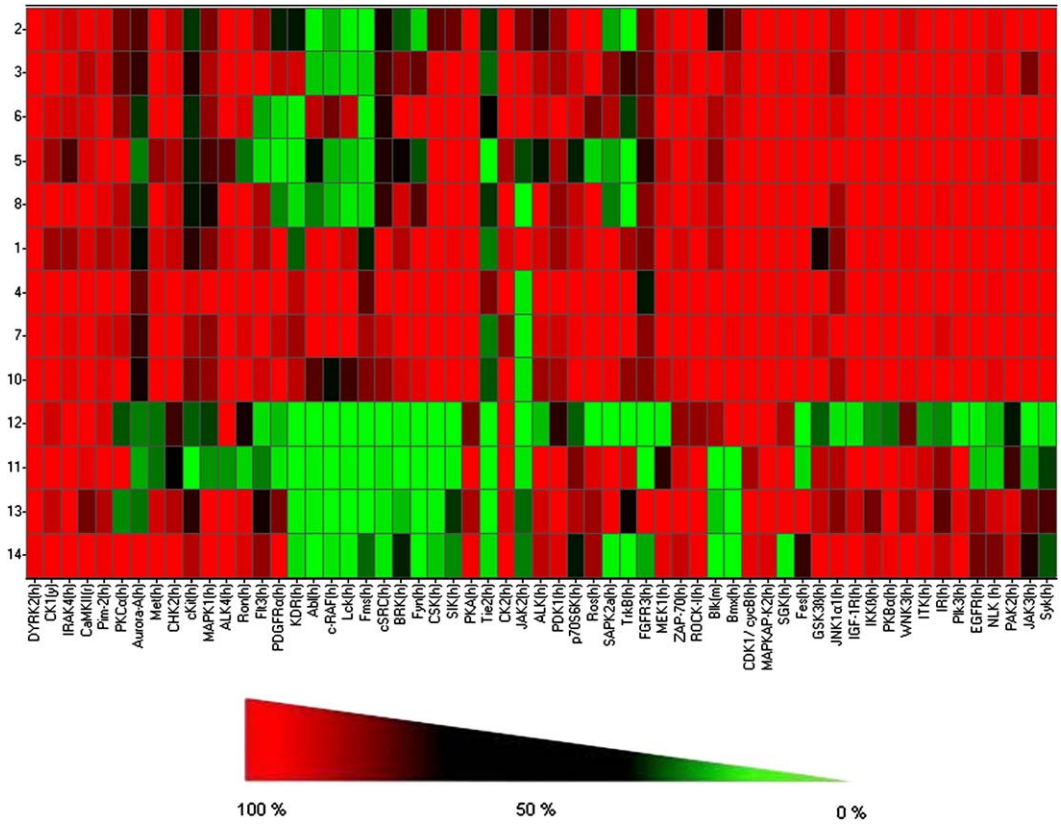

Figure 3. Heat Map for the Percentage of Kinase Inhibitory Activity for Compounds **1–14**, with the Exception of **9**

Compounds **1–11**, **13**, and **14** were assayed at 1 μM, and compound **12** was assayed at 10 μM. Color gradation is proportional to the percentage of activity remaining: Green = inhibited; red = not inhibited.

visualized in Figure 4 (IC_{50} values are reported in the Supplemental Data available with this article online, see Table S1). For example, inhibitors **2**, **5**, **8**, **12**, and **14** all displayed sub-100 nM activity against cellular PDGFR-β, while **2**, **8**, **12**, and **14** targeted Bcr-Abl with IC_{50}s in the 3–110 nM range. Type II inhibitor **6** displayed a unique and selective inhibitory profile of Flt3, c-Kit, and PDGFR-α/β. Another notable change in the selectivity profile is demonstrated by the replacement of 2-methyl substituent of **8** with a 3-methoxy group of **9** that possesses a sub-100 nM cellular IC_{50} exclusively against c-Kit. The two-dimensional hierarchical clustering also reveals that the 3-trifluoromethylbenzamide "tail" portion of these inhibitors exhibited a dominant effect on the overall kinase selectivity. This is demonstrated by the proximal clustering of **2** and **8** and **3** and **6**, where the hinge region interacting motifs are structurally quite different. The results show that the designed type II inhibitors can potently inhibit the cellular activity of different subsets of tyrosine kinases.

SAR for Amide and Urea Modifications

To investigate the importance of the amide (or urea for **5**) NH to serve as a hydrogen bond donor, the corresponding N-methyl (**3**, **10**, **13**, and **15**) or CH_2 (**6**) replacements were prepared and tested for cellular kinase inhibition. As expected from the design strategy, both compounds **3** and **10** exhibited approximately a 100-fold loss in cellular activity on Bcr-Abl and PDGFR-β, while **13** lost activity on ALK, Bcr-Abl, BMX, EphA3, EphB4, and a host of other kinases. Interestingly, compound **6** lost activity on KDR, and there was a decrease in activity on several other kinases as well. However, activity on PDGFR-β was maintained potentially due to the ability of the other urea NH to provide an alternative hydrogen bond donor. These results show that the urea or amide NH is essential for potent cellular inhibition of the newly designed type II inhibitors, and this finding is consistent with the binding mode predicted by the design strategy.

Biochemical Inhibition of Differentially Phosphorylated Abl

It has been previously demonstrated that imatinib possesses a lower IC_{50} for inhibition of the activation loop-dephosphorylated Abl than for fully phosphorylated Abl [8, 9]. This is presumed to result from imatinib's preference for binding to the activation loop-dephosphorylated Abl, which can preferentially assume the DFG-out conformation. In order to determine IC_{50}s against phosphorylated (more active) and dephosphorylated (less active) Abl kinases, we established an in vitro kinase assay by using either phosphorylated or dephosphorylated recombinant human Abl kinase domains to phosphorylate a peptide substrate. Using this assay, imatinib was demonstrated to be ~85-fold more potent on dephosphorylated compared to phosphorylated Abl.

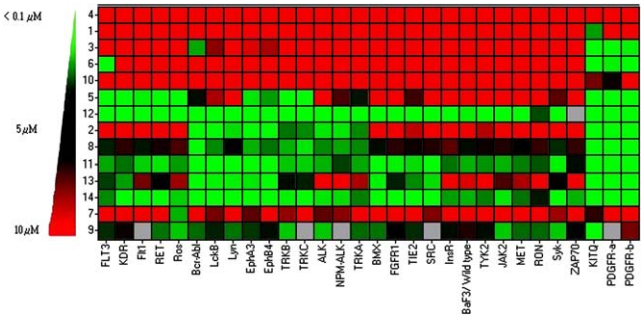

Figure 4. Heat Map for Antiproliferative IC_{50}s, in μM, of Compounds **1**–**14** on Parental and Kinase-Transformed Ba/F3 Cells

Gray = not tested.

In contrast, the known type I inhibitor PD173955 was equipotent in both assays (Table 2) [8]. As expected from the design strategy, the type II compounds **2**, **5**, and **8** exhibited several fold lower IC_{50}s for the dephosphorylated Abl. In line with our expectations, the control compounds **3**, **6**, and **10** were all inactive in the biochemical assay. These results would suggest that compounds **2**, **5**, and **8** are able to preferentially bind and inhibit the dephosphorylated inactive Abl conformation compared with phosphorylated active Abl. In contrast to our expectations, type II analogs **12** and **14** did not exhibit any differential in activity with respect to the phosphorylation state of the Abl enzyme. The exceptional potency of **12** and **14** may be sufficient to drive the conformational equilibrium in favor of the DFG-out state regardless of the phosphorylation status of the kinase. Unlike compound **13**, N-Me analog **15** showed no activity of Abl in either the phosphorylated state or the dephosphorylated state. This result might be explained by the fact that **13** has an optimized type I inhibitor region; hence, modification of amide linkage in the allosteric pocket has a minimal effect on the potency of the molecule.

Crystal Structure of 14 with Abl

In an effort to determine the inhibitor bound conformation of Abl, we solved the cocrystal structure with a simplified structural analog of compound **12** (**14**) to a resolution of 2.3 Å (Figure 5). Compound **14** was used instead of **12** because of its enhanced water solubility and similar biological profile in both biochemical and cellular kinase assays (Tables 1 and 2; Table S1). The cocrystal structure revealed that compound **14** indeed utilizes a type II binding mode to Abl; the activation loop in the DFG-out conformation is highly reminiscent of Abl bound to imatinib or nilotinib (AMN-107) [32]. Furthermore, the cocrystal showed all of the expected inhibitor-protein interactions predicted by the design strategy: a pair of hydrogen bonds to the kinase hinge (residue Met318) from the aminopyrimidine motif, a twisted conformation of the tolyl moiety, two hydrogen bonds from the amide to the side chain of Glu286 in the α-C helix and to the backbone amide of D381 in the DFG motif. A superposition with imatinib revealed the high degree of molecular mimicry between the two compounds. Based on data available from kinase cocrystal structures of nilotinib with Abl (analog of **2**), sorafenib with b-Raf (analog of **5**), and **14** with Abl, one can see that all compounds exhibit the conserved features of the type II binding mode. All costructures exhibit the DFG-out conformation of the activation loop and two pairs of conserved hydrogen bonds: one pair binds to the hinge region amino acid, and a second pair binds to the side chain carboxylate of a conserved glutamate in the α-C helix and to the backbone NH of the aspartate in the DFG motif in the allosteric region.

Discussion

There is an ever-increasing demand for new protein kinase inhibitors both as potential therapeutics and as tools to aid in dissecting complex signaling pathways. Despite the tremendous efforts to develop new kinase inhibitors, the vast majority of kinases are still not targeted by an inhibitor with a reasonable level of selectivity. Currently, the majority of known small-molecule kinase inhibitors exclusively target the ATP binding site of the fully activated kinase (type I inhibitors). A second class of inhibitors (type II inhibitors) that exploit a hydrophobic pocket immediately adjacent to the ATP binding site created by a unique DFG-out conformation of the activation loop characteristic of an inactive kinase was subsequently identified. Because type II inhibitors recognize regions of the kinase active cleft outside of the highly conserved ATP binding site, they have been predicted to have the potential to exhibit a higher degree of kinase selectivity. To date, all of the known type II inhibitors have been identified serendipitously and were only later determined to be type II binders through examination of X-ray costructures. By inspecting the inhibitor bound conformations of all type II inhibitors for which

Table 2. IC_{50s}, in nM, of Type II Inhibitors on Phosphorylated and Dephosphorylated Abl

Inhibitor	Phosphorylated Abl	Dephosphorylated Abl
Imatinib	>5000	27.0
PD173955	24.0	23.0
1	>5000	>5000
2	152	5
3	>5000	1362
4	>5000	>5000
5	>5000	374
6	>5000	>5000
7	>5000	>5000
8	>5000	154
10	>5000	>5000
11	5.7	5.8
12	19.6	27.2
13	150.1	9.1
14	11.0	8.0
15	>5000	>5000

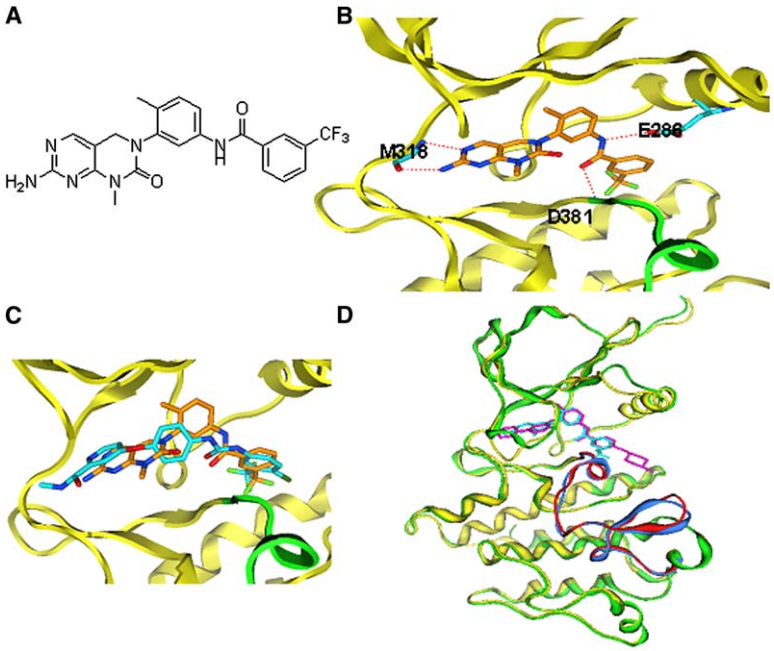

Figure 5. Crystal Structure of Compound **14** Bound to Abl

(A) Chemical structure of compound **14**.
(B) H-bonding interactions of compound **14** with Abl ATP site residues.
(C) Superimposition of compound **14** and soranefib bound to Abl.
(D) Ribbon diagram of Abl kinase in the presence of imatinib and compound **14**.

there are known kinase cocrystal structures, we were able to derive a general pharmacophore model.

This pharmacophore model suggests that grafting a 3-trifluoromethylbenzamide moiety to the appropriate position on a type I inhibitor would provide a simple strategy for synthesizing new type II inhibitors. We exploited this approach to prepare four distinct classes of type II inhibitors (**2**, **5**, **8**, **9**, **12**, and **14**) from known type I inhibitors (**1**, **4**, **7**, and **11**). For all four compound pairs, the type II inhibitors were more capable of inhibiting the enzymatic activity of a larger number of kinases than their corresponding type I counterparts at concentrations of 1 or 10 μM. This is likely to result from a combination of changes in inhibitor potency and selectivity: type II inhibitors can display lower IC_{50}s for certain kinases and/or possess the ability to inhibit fundamentally distinct kinases compared to type I inhibitors. The comparison of kinase selectivity between type I and II inhibitors needs to be performed on a larger set of inhibitors before any general conclusion can be drawn. With the exception of **11**, the type I inhibitors used as starting scaffolds in this work (**1**, **4**, and **7**) are not potent kinase inhibitors; consequently, this makes them appear to be selective.

In contrast to previously described type II inhibitors, we have demonstrated that it is possible to make type II inhibitors such as **12** and **14** that are exceptionally potent and nonselective kinase inhibitors. This demonstrates that despite the ability of these inhibitors to exploit the less-conserved allosteric pocket, their overall mode of kinase binding can be sufficiently generic such that the desired kinase selectivity is not achieved. However, we have also shown that the selectivity of the type II compounds can be dramatically enhanced by very subtle chemical alterations, as exemplified by compounds **6** and **9**. Similarly, modification in compound **11** led to nonselective type II analog **12** or to a more selective compound, **14**. We demonstrated that for the compounds with nonoptimized hinge contact for which Bcr-Abl was a target (**2**, **5**, and **8**), the type II inhibitors displayed a significantly lower IC_{50} against dephosphorylated Abl enzyme. This result suggests that the type II inhibitors are capable of accessing a more productive inhibitory conformation when the kinase is dephosphorylated, in contrast to type I inhibitors, for which this discrimination is not apparent. Moreover, the type II scaffolds are demonstrated to target a spectrum of kinases that can be restricted based on subtle alterations to the chemical structure, as exemplified by **5** versus **6** and **8** versus **9**.

When tested for the inhibition of cell proliferation dependent on a panel of 30 tyrosine kinases, all 4 classes of type II inhibitors displayed potent cellular activity against one or more tyrosine kinases. This was in stark contrast to the four type I inhibitor classes for which only the pyrimidopyrimidone **11** displayed potent cellular activity against a large number of tyrosine kinases. From the cocrystal structures obtained of compound **14** and Abl, we were able to conclusively demonstrate that this compound does indeed bind to the DFG-out Abl conformation, as has been observed for imatinib and nilotinib. The remarkable cellular activity of the type II inhibitors may result from their binding to the inactive conformation of the kinases, which may be more accessible in the cellular environment.

A key challenge to furthering the development of new type II inhibitors as therapeutic leads is to develop a detailed understanding of how structural modifications impact kinase selectivity. This will require preparing a variety of structural analogs in order to explore cellular structure-activity against a panel of kinases. An example of such a modification is the replacement of the urea NH of compound **5** with a methylene to form compound **6**, which results in a significant improvement of kinase selectivity. Additional challenges include finding effective strategies for increasing the solubility and pharmacokinetic properties of compounds containing the highly lipophilic 3-trifluoromethylbenzamide substituent.

As most currently known kinase inhibitors are type I, it is likely that the technique we describe here will provide a simple rational way to construct a large number of type II inhibitor counterparts that will display distinct kinase selectivity profiles and exceptional cellular potency. The ability to readily achieve extraordinary cellular potency against a diverse assortment of kinase targets will likely make this strategy for creating new type II inhibitors popular for both the development of therapeutic lead compounds and for making "tool" compounds for pharmacological interrogation of cellular signaling networks.

Significance

Tremendous effort is being invested in the discovery of protein kinase inhibitors for the treatment of a number of human diseases. Although 5 distinct small-molecule kinase inhibitors have been approved for the treatment of specific cancers and over 100 agents are under clinical evaluation, the vast majority of kinases are still not targeted by an inhibitor with a useful level of selectivity [33]. There is therefore a compelling need to expand the diversity of small-molecule scaffolds that can be tuned to the desired selectivity profile. Here, we describe a simple chemical strategy that can be applied to transform the large number of compounds that are known to target the ATP binding pocket of active kinases (type I) [34, 35] into inhibitors that can exploit an additional hydrophobic binding site available in the DFG-out conformation (type II). The hybrid-design approach involves grafting functionality from known type II inhibitors onto type I scaffolds. By targeting the DFG-out conformation, the resulting type II hybrid compounds can exhibit exceptional cellular potency and can serve as starting points for elaboration of compounds with a range of selectivity profiles that can serve as leads for drug discovery or as pharmacological probes of signaling pathways.

Experimental Procedures

Generation of Tyrosine Kinase-Transformed Ba/F3 Cells

Kinase domains (KD) of tyrosine kinases were individually PCR amplified from a human cDNA library, subsequently cloned into a modified pMSCVpuro vector (Clontech), and transduced into Ba/F3 cells as previously described [31]. Expression of tyrosine kinases in transduced Ba/F3 cells was confirmed by immunodetection of the Tel-KD fusion proteins and by sequence analysis of RT-PCR products.

Ba/F3 Cell Proliferation Assay

Ba/F3 cells transformed by tyrosine kinases were dispensed into a 384-well format plate at 5000 cell/well in 50 μl culture medium. Twelve point serial dilutions of the test compounds in DMSO were transferred into cell plates to final compound concentration gradients ranging from 0.05 to 10,000 nM. After incubation at 37°C in 5% CO_2 for 48 hr, relative cell numbers for each compound treatment were determined by measuring the luminescent signal resulting from addition of the luciferase substrate Bright-Glo (Promega). IC_{50} values are calculated by linear regression analysis of the percent inhibition of each compound at 12 concentrations.

Phosphorylated and Dephosphorylated Kinase Assay

Dephosphorylated conformationally inactive Abl kinase was obtained by treating pure recombinant Abl with *Yersinia enterocolitica* phosphatase (Calbiochem) (50 U/μg Abl) in the appropriate buffer (100 mM Tris [pH 7.5], 150 mM NaCl, 2.5 mM EDTA, 5 mM DTT) for 30 min at 30°C. The tyrosine phosphorylation status of the enzyme was assessed by immunoblotting with anti-phosphotyrosine antibody (4G10 clone, Upstate). After addition of Na_3VO_4 at a final concentration of 2 mM to inhibit phosphatase activity, nontreated and dephosphorylated Abl were incubated with various concentrations of test compounds in kinase buffer (50 mM Tris-HCl [pH 7.5], 10 mM $MgCl_2$, 100 mM EDTA, 1 mM DTT, 0.015% Brij 35), 150 μM Abl substrate peptide (Upstate), 100 μM ATP, and 1 μCi [γ-^{33}P]-ATP. Assays were carried out in 96-well plates at room temperature for 30 mi, and 35 μl of the reaction mixture was transferred onto 96-well phosphocellulose membrane plates (Millipore, Bedford, MA) previously soaked with 0.5% H_3PO_4 and mounted on a vacuum manifold. Membranes were washed five times with 1.0% H_3PO_4, and, after addition of 10 μl/well of Microscint TM (Packard), the radioactivity incorporated into the substrate was quantified in a Packard Top Count. The IC_{50} value was calculated by linear regression analysis of the percent inhibition curve (see the curves and the Western blot in the Supplemental Data). The assay typically has an S/N ratio of 30:1 or higher.

Supplemental Data

Supplemental Data include experimental details for the synthesis of compounds, details on cocrystallization of **14** with c-Abl, and raw data of heat maps that are included in the main text and are available at http://www.chembiol.com/cgi/content/full/13/7/779/DC1/.

Acknowledgments

We acknowledge expert technical assistance from Xiang-ju Gu, Ansgar Brock, Tami Hood, Sungjoon Kim, Feng Gao, Haiyan Xu, Alham Saadat, Vicki Wei Zhou, Andreas Kreusch, and Tammy Colbert.

Received: April 14, 2006
Revised: May 23, 2006
Accepted: May 30, 2006
Published: July 28, 2006

References

1. Manning, G., Whyte, D.B., Martinez, R., Hunter, T., and Sudarsanam, S. (2002). The protein kinase complement of the human genome. Science *298*, 1912–1934.
2. Blume-Jensen, P., and Hunter, T. (2001). Oncogenic kinase signalling. Nature *411*, 355–365.
3. Cohen, P. (2002). Protein kinases—the major drug targets of the twenty-first century? Nat. Rev. Drug Discov. *1*, 309–315.
4. Dancey, J., and Sausville, E.A. (2003). Issues and progress with protein kinase inhibitors for cancer treatment. Nat. Rev. Drug Discov. *2*, 296–313.
5. Hunter, T. (1998). The role of tyrosine phosphorylation in cell growth and disease. Harvey Lect. *94*, 81–119.
6. Traxler, P., and Furet, P. (1999). Strategies toward the design of novel and selective protein tyrosine kinase inhibitors. Pharmacol. Ther. *82*, 195–206.
7. Hubbard, S.R., Wei, L., Ellis, L., and Hendrickson, W.A. (1994). Crystal structure of the tyrosine kinase domain of the human insulin receptor. Nature *372*, 746–754.
8. Nagar, B., Bornmann, W.G., Pellicena, P., Schindler, T., Veach, D.R., Miller, W.T., Clarkson, B., and Kuriyan, J. (2002). Crystal structures of the kinase domain of c-Abl in complex with the small molecule inhibitors PD173955 and imatinib (STI-571). Cancer Res. *62*, 4236–4243.
9. Schindler, T., Bornmann, W., Pellicena, P., Miller, W.T., Clarkson, B., and Kuriyan, J. (2000). Structural mechanism for STI-571 inhibition of abelson tyrosine kinase. Science *289*, 1938–1942.
10. Mol, C.D., Fabbro, D., and Hosfield, D.J. (2004). Structural insights into the conformational selectivity of STI-571 and related kinase inhibitors. Curr. Opin. Drug Discov. Devel. *7*, 639–648.
11. Pargellis, C., Tong, L., Churchill, L., Cirillo, P.F., Gilmore, T., Graham, A.G., Grob, P.M., Hickey, E.R., Moss, N., Pav, S., et al. (2002). Inhibition of p38 MAP kinase by utilizing a novel allosteric binding site. Nat. Struct. Biol. *9*, 268–272.
12. Wan, P.T., Garnett, M.J., Roe, S.M., Lee, S., Niculescu-Duvaz, D., Good, V.M., Jones, C.M., Marshall, C.J., Springer, C.J., Barford, D., et al. (2004). Mechanism of activation of the

RAF-ERK signaling pathway by oncogenic mutations of B-RAF. Cell *116*, 855–867.

13. Manley, P.W., Bold, G., Bruggen, J., Fendrich, G., Furet, P., Mestan, J., Schnell, C., Stolz, B., Meyer, T., Meyhack, B., et al. (2004). Advances in the structural biology, design and clinical development of VEGF-R kinase inhibitors for the treatment of angiogenesis. Biochim. Biophys. Acta *1697*, 17–27.
14. Gill, A.L., Frederickson, M., Cleasby, A., Woodhead, S.J., Carr, M.G., Woodhead, A.J., Walker, M.T., Congreve, M.S., Devine, L.A., Tisi, D., et al. (2005). Identification of novel p38α MAP kinase inhibitors using fragment-based lead generation. J. Med. Chem. *48*, 414–426.
15. Cumming, J.G., McKenzie, C.L., Bowden, S.G., Campbell, D., Masters, D.J., Breed, J., and Jewsbury, P.J. (2004). Novel, potent and selective anilinoquinazoline and anilinopyrimidine inhibitors of p38 MAP kinase. Bioorg. Med. Chem. Lett. *14*, 5389–5394.
16. Heron, N.M., Anderson, M., Blowers, D.P., Breed, J., Eden, J.M., Green, S., Hill, G.B., Johnson, T., Jung, F.H., McMiken, H.H., et al. (2006). SAR and inhibitor complex structure determination of a novel class of potent and specific Aurora kinase inhibitors. Bioorg. Med. Chem. Lett. *16*, 1320–1323.
17. Dudley, D.T., Pang, L., Decker, S.J., Bridges, A.J., and Saltiel, A.R. (1995). A synthetic inhibitor of the mitogen-activated protein kinase cascade. Proc. Natl. Acad. Sci. USA *92*, 7686–7689.
18. Duncia, J.V., Santella, J.B., 3rd, Higley, C.A., Pitts, W.J., Wityak, J., Frietze, W.E., Rankin, F.W., Sun, J.H., Earl, R.A., Tabaka, A.C., et al. (1998). MEK inhibitors: the chemistry and biological activity of U0126, its analogs, and cyclization products. Bioorg. Med. Chem. Lett. *8*, 2839–2844.
19. Sebolt-Leopold, J.S., Dudley, D.T., Herrera, R., Van Becelaere, K., Wiland, A., Gowan, R.C., Tecle, H., Barrett, S.D., Bridges, A., Przybranowski, S., et al. (1999). Blockade of the MAP kinase pathway suppresses growth of colon tumors in vivo. Nat. Med. *5*, 810–816.
20. Martinez, A., Alonso, M., Castro, A., Perez, C., and Moreno, F.J. (2002). First non-ATP competitive glycogen synthase kinase 3 beta (GSK-3β) inhibitors: thiadiazolidinones (TDZD) as potential drugs for the treatment of Alzheimer's disease. J. Med. Chem. *45*, 1292–1299.
21. Burke, J.R., Pattoli, M.A., Gregor, K.R., Brassil, P.J., MacMaster, J.F., McIntyre, K.W., Yang, X., Iotzova, V.S., Clarke, W., Strnad, J., et al. (2003). BMS-345541 is a highly selective inhibitor of I κ B kinase that binds at an allosteric site of the enzyme and blocks NF-κ B-dependent transcription in mice. J. Biol. Chem. *278*, 1450–1456.
22. Adrian, F.J., Ding, Q., Sim, T., Velentza, A., Sloan, C., Liu, Y., Zhang, G., Hur, W., Ding, S., Manley, P., et al. (2006). Allosteric inhibitors of Bcr-abl-dependent cell proliferation. Nat. Chem. Biol. *2*, 95–102.
23. Barnett, S.F., Defeo-Jones, D., Fu, S., Hancock, P.J., Haskell, K.M., Jones, R.E., Kahana, J.A., Kral, A.M., Leander, K., Lee, L.L., et al. (2005). Identification and characterization of pleckstrin-homology-domain-dependent and isoenzyme-specific Akt inhibitors. Biochem. J. *385*, 399–408.
24. Gumireddy, K., Reddy, M.V., Cosenza, S.C., Boominathan, R., Baker, S.J., Papathi, N., Jiang, J., Holland, J., and Reddy, E.P. (2005). ON01910, a non-ATP-competitive small molecule inhibitor of Plk1, is a potent anticancer agent. Cancer Cell *7*, 275–286.
25. Zimmermann, J., Buchdunger, E., Mett, H., Meyer, T., and Lydon, N. (1997). Potent and selective inhibitors of the Abl-kinase: phenylamino-pyrimidine (PAP) derivatives. Bioorg. Med. Chem. Lett. *7*, 187–192.
26. Wang, S., Meades, C., Wood, G., Osnowski, A., Anderson, S., Yuill, R., Thomas, M., Mezna, M., Jackson, W., Midgley, C., et al. (2004). 2-Anilino-4-(thiazol-5-yl)pyrimidine CDK inhibitors: synthesis, SAR analysis, X-ray crystallography, and biological activity. J. Med. Chem. *47*, 1662–1675.
27. Changelian, P.S., Flanagan, M.E., Ball, D.J., Kent, C.R., Magnuson, K.S., Martin, W.H., Rizzuti, B.J., Sawyer, P.S., Perry, B.D., Brissette, W.H., et al. (2003). Prevention of organ allograft rejection by a specific Janus kinase 3 inhibitor. Science *302*, 875–878.
28. Chen, J.J., Dewdney, N.J., and Stahl, C.M. (2003). Bicyclic pyridine and pyrimidine derivatives, e.g., thieno[2,3-d]pyrimidines and analogs, active as p38 kinase inhibitors, and their preparation, pharmaceutical compositions, and uses. Switzerland patent WO2003074530.
29. Klutchko, S.R., Hamby, J.M., Boschelli, D.H., Wu, Z., Kraker, A.J., Amar, A.M., Hartl, B.G., Shen, C., Klohs, W.D., Steinkampf, R.W., et al. (1998). 2-Substituted aminopyrido[2,3-d]pyrimidin-7(8H)-ones. Structure-activity relationships against selected tyrosine kinases and in vitro and in vivo anticancer activity. J. Med. Chem. *41*, 3276–3292.
30. Martinelli, G., Soverini, S., Rosti, G., and Baccarani, M. (2005). Dual tyrosine kinase inhibitors in chronic myeloid leukemia. Leukemia *19*, 1872–1879.
31. Melnick, J.S., Janes, J., Kim, S., Chang, J.Y., Sipes, D.G., Gunderson, D., Jarnes, L., Matzen, J.T., Garcia, M.E., Hood, T.L., et al. (2006). An efficient rapid system for profiling the cellular activities of molecular libraries. Proc. Natl. Acad. Sci. USA *103*, 3153–3158.
32. Manley, P.W., Cowan-Jacob, S.W., and Mestan, J. (2005). Advances in the structural biology, design and clinical development of Bcr-Abl kinase inhibitors for the treatment of chronic myeloid leukaemia. Biochim. Biophys. Acta *1754*, 3–13.
33. Klebl, B.M., and Muller, G. (2005). Second-generation kinase inhibitors. Expert Opin. Ther. Targets *9*, 975–993.
34. Noble, M., Barrett, P., Endicott, J., Johnson, L., McDonnell, J., Robertson, G., and Zawaira, A. (2005). Exploiting structural principles to design cyclin-dependent kinase inhibitors. Biochim. Biophys. Acta *1754*, 58–64.
35. Pratt, D.J., Endicott, J.A., and Noble, M.E. (2004). The role of structure in kinase-targeted inhibitor design. Curr. Opin. Drug Discov. Devel. *7*, 428–436.